EXPERIMENTAL INVESTIGATION ON THE IMPACT OF CONCRETE STRENGTH ON THE DUCTILITY OF REINFORCED CONCRETE FRAME STRUCTURES

Lieutenant Colonel Bhuiyan Mohammad Golam Kibria

Course member AFWC 2019
National Defence Colloge, Mirpur Cantonment, Mirpur-12, Dhaka-1216
E-mail: kibria1976@gmail.com

ABSTRACT

This experiment was undertaken to study the impact of concrete strength on the ductility of reinforced concrete frame structure. Two half scale interior joint with monolithic transverse beams and slab from a six storied residential building were selected for the experiment. The joints were constructed without any shear reinforcement within the joint region to evaluate the contribution of concrete strength in bond stress between the longitudinal reinforcement and concrete. Bond stress has important specific roles on the ductility of the joint in particular and on the ductility of the global structure in general. The models were subjected to incremental static cyclic lateral loading provided by hydraulic jacks under constant axial loading. Deflections and rotations were measured by dial gauges and a video extensometer. It is found from the study that ductility of the structural members i.e. beams, columns and joints increased remarkably with increased concrete strength.

Key words: Concrete strength, ductility, interior joint, seismic loading

ACKNOWLEDGEMENT

The authors express their deep appreciation to KSRM, Seven Circles (Bangladesh) Limited, Nutech Construction Chemicals Company Limited and Bangladesh Building Systems Limited for their material and technical support. The authors convey their gratitude to Bangladesh Army for financial grants and support in doing the experimental works. The authors also express their gratitude to all members of Concrete Laboratory, Civil Engineering Department, BUET for all types of material and technical supports. It would not be possible to complete the experiments without their assistance.

1.0 INTRODUCTION

Ductility is defined as the ability of a material to undergo large deformation without rupture before failure. Ductility can be defined with respect to strain, rotations, curvature and deflections. Strain based ductility definition depends on material while rotation and curvature depends on shape and size of the cross sections as well. Global ductility of the overall structure is derived from local ductility of structural members. In seismic design philosophy, the structures should have sufficient ductility to dissipate seismic energy. If a structure is ductile then it can undergo large deformations without rupture before failure and will provide warning to the occupants. There are desired locations where structural damage is allowed to occur (ACI 2004, FEMA 273) which is called plastic hinges. Structural failure must not occur at the columns as failure in this region make the stability of the entire structure vulnerable and may lead to a catastrophic failure of the structure. Beam-column joints are at the intermediate level of strength hierarchy. The joint behavior exhibits a complex interaction between bond and shear. The forces acting in the joints and failure mechanism under seismic events are discussed in many literatures. Earthquake or seismic loading induces large shear stresses in the joint region by. Combined effect of the shear stresses causes diagonal cracking when tensile stress exceeds the tensile strength of the concrete. Extensive cracking occurs due to load reversals under seismic event. The joints should be strengthened to move the failure to the beams. Such failure would be the best result for seismic upgrade and this means that very efficient ductile and energy dissipating mechanism is achieved which would maintain global integrity of the structure (Prota et al. 2004). The joint performance can be enhanced by proper seismic detailing and ensuring proper concrete confinement in joint region. As it is said that the structural ductility comes from the member ductility and member ductility is gained through the inelastic rotations. In seismic design, it is desired that the plastic hinges should occur at beams rather than in the columns (FEMA 273, Akguzel et al. 2007). It leads to the Strong Column-Weak Beam Strategy which can be achieved by proper detailing in columns, beams and at the joints. On the other hand, functional requirement of a joint, which is the zone of intersection of beam and columns, is to enable the adjoining members to develop and sustain their ultimate capacity. The joints should have adequate strength and stiffness to sustain the forces induced by the adjoining members. Detailing of the shear reinforcement in seismic design is discussed in various national and international codes. This experiment is undertaken to understand the roles of concrete strength on the overall ductility of the Reinforced Concrete (RC) Framed structures. An interior joint of a Six Storied Residential building is selected for the study.

2.0 MATERIAL PROPERTIES

2.1 Sand

Coarse Sylhet sand and fine river sands were used for all specimens of the present experiment. Two batches of sands were prepared for model preparation. Sylhet Sand and local river sand were mixed in 3:1 proportion as it is done in most of the construction works in Bangladesh. Absorption capacity of the sand samples was 4% but moisture contents varied widely due to monsoon rain. Moisture content of the aggregates was measured before mixing and water content of the fresh concretes was adjusted accordingly. Fineness Modulus (FM) values of two batches of mixed sands were found 2.64 and 2.71 respectively by sieve analysis. Gradations of the samples are shown in Fig.1.

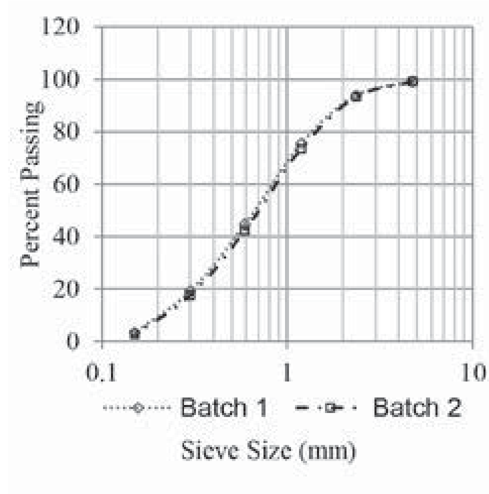

Fig 1. Grade of Fine Aggregates

2.2 Coarse Aggregate

The compressive strength of crushed stone aggregates is higher and provides better compressive strength of the concrete as well but 1st class 'Jhama' bricks having average compressive strength 26.29 MPa or 3810 psi were used for casting the models. Most of the buildings in Bangladesh are still constructed by coarse aggregates made from crushing the 'Jhama' bricks. Therefore, 10 mm down grade brick chips made from crushing first class bricks by hand were collected for model preparation. Specific gravity and absorption capacity of the coarse aggregate were 1.93 and 17.98% respectively.

2.3 Cement

For controlled and strengthened specimens Portland Cement CEM-I was used. The properties of the cement are given in Table 1.

Table1. Properties of Cement

Properties	**Unit**		
Setting Time (ASTM C191)	Minute		
Initial Setting Time		> 45	129
Final Setting Time		<375	266
Strength (ASTM C109)	MPa		
3 Days		> 12	24.95
7 Days		>19	35.20
28 Days		> 28	42.85

2.4 Reinforcement

Φ12 mm and Φ8 mm Grade 60/400 steel reinforcement was used for model construction in this experiment. Samples were tested for yield and ultimate capacity. The test results are given in Table 2.

Table 2. Strength of Reinforcing Bars

Dia (mm)	Elongation (%)	Bar Area (mm^2)	Yield Strength (MPa)	Ultimate Strength (MPa)
12	15.67	114.1	444	749
8	18	50.8	429	657

3.0 MODEL PREPARATION AND EXPERIMENTAL SET UP

3.1 Model Selection

The models were selected considering a full scale six storied RC Frame Structured Building as shown in Fig.2. The story height of the building was 3100 mm and bay width was 4000 mm. The building was analyzed by ETABS 9.7 following ACI 318-05/IBC-2003. An interior joint from Storey-3 of the building was selected for the experimental program as shown in Fig.2. Considering the existing laboratory set up half scale model was selected. Dimensions of the half scale model are shown in Fig.3 and Fig.4. Dimensions and detailing of beam and column of the models are shown in Fig. 5 and Fig.6. The beams of the models had been made stronger than the column to observe the behavior of column failure.

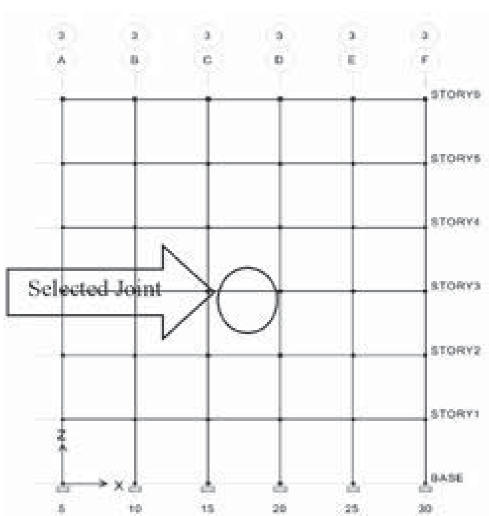

Fig 2. Global Structure

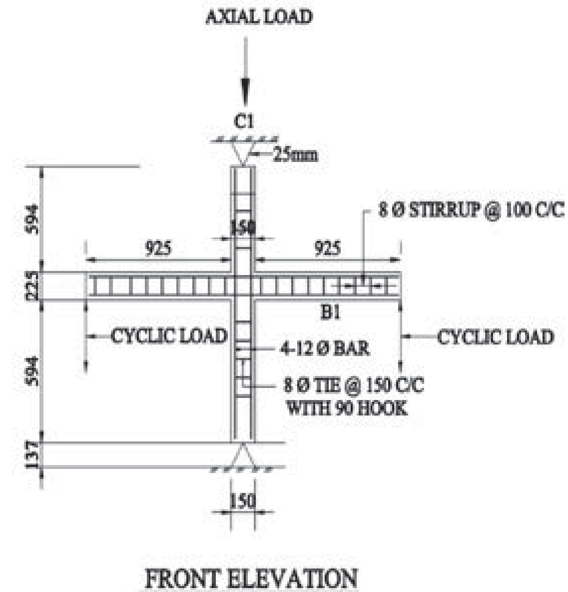

Fig 3. Dimensions of as Built Half Models

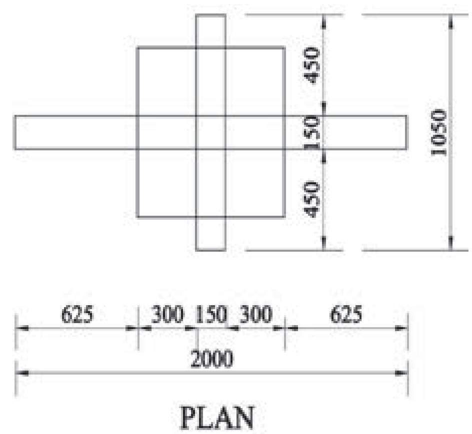

Fig 4. Plan View of as Built Half Models

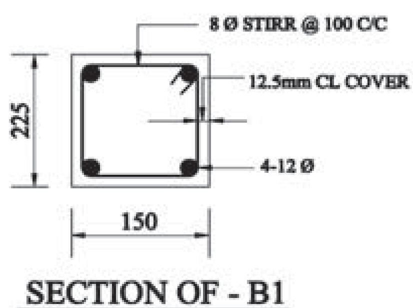

Fig 5. Details of Reinforcement of Beam

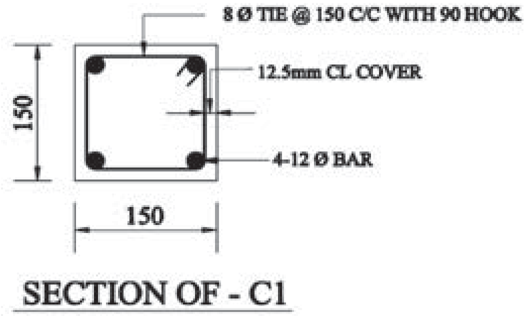

Fig 6. Details of Reinforcement of Column

3.2 Model Preparation

Two models were constructed for this experiment. The model will be designated as Model 1 and Model 2 in subsequent discussions. The model with lesser concrete strength is termed as Model 1 and the model with higher concrete strength is termed as Model 2. The form works, made of woods and ply woods, were used for casting the models. Lower column, beams and slabs were cast together as shown in Fig.7.

Fig 7. Concrete Casting of the Models

Water contents of fresh concretes were controlled by slump value to ensure better workability. Slump value varied between 50-75 mm. W/c ratios of Model 1 and Model 2 were 0.58 and 0.51 respectively. Fresh concretes were mechanically compacted. The models were cured for 28 days by wet jute cloth. To minimize the loss of moisture from the models, the formworks (Shuttering) were kept for 28 days. Average concrete strengths of Model 1 and Model 2 were found 18.31 MPa (2600 psi) and 28.31 MPa (4000 psi) respectively from the cylinder tests. Concrete strength of Model 2 was 54% more than that of Model 1.

3.3 Experimental Set Up

The models were placed on a steel base plate which had the arrangement of column seat. The base plate was intended to allow column rotation by incorporating roller at the bottom as shown in Fig.8.

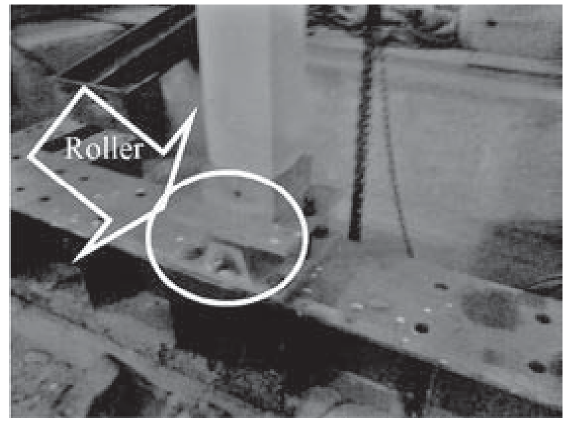

Fig 8. Hinge Joint for Column Rotation

The base plate was fixed on a steel 'I-Beam' which was fixed with the concrete floor. A 50 kN capacity hydraulic jack was used to provide axial load on the column. Two manually operated hydraulic jacks were used to provide cyclic loading near the tip of the beams. Two sets of steel frames were designed for this experiment. They were fixed on both side of the column to arrest any horizontal movement of the column. A schematic view of the experimental set up is shown in Fig.9 and a detail view is shown in Fig.10.

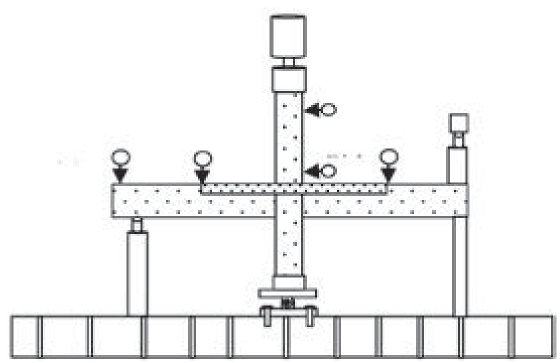

Fig 9. Schematic View of Experimental Set Up

Five dial gauges were used to measure the deflection of the beams and columns. First two dial gauges were set near the tip and at the beam-slab joint of the left beam. One dial gauge was fixed at the beam-slab joint of the right beam. Another two dial gauges were set at 10 cm below the column top and at 10 cm above the column-slab joint of the top column. Video extensometer was used to measure the rotation of the beam and column at the joint region. Video extensometer was placed closed to the joint. "+" markings on the joint, as shown in the Fig.11, were used as the target to measure the beam and column joint rotation. The mark on the wooden plank was used to measure the absolute rotation of the specified target.

Fig 10. Detail View of Experimental Set Up

3.4 Load Selection

Strength of beam-column joint is influenced by the effective confinement of concrete. Column axial load also increases the confinement. To understand the behavior of all joints under identical condition, constant axial load of 10% of the column capacity (0.1fc´Ag) was applied. Axial loads for Model 1 and Model 2 were 45 and 65 kN respectively.

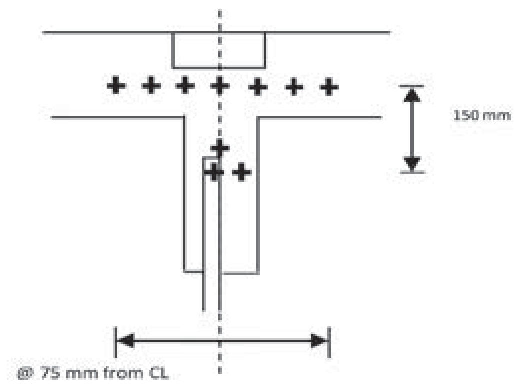

Fig 11. Schematic Diagram of Target for Video Extensometer

The static incremental cyclic loading was applied by two manually operated hydraulic jacks. The loading was controlled by measuring the column drift of the column top. 0.25%, 0.50%, 1% and 2% of the column drift were selected as the points of reversal for cyclic loading. Minimum division of the dial of hydraulic jacks was 5 kN (0.5 ton). Therefore, loading and unloading rate was 5 kN in a single increment. However, as the jacks were manually operated, loading and unloading could not be maintained at the same rate which may have influenced the result due to visco-elastic effect. The load cycles are shown in Fig .12.

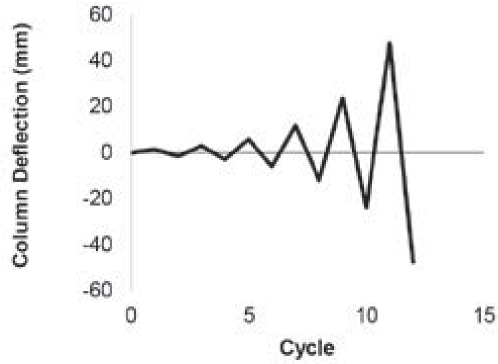

Fig 12. Loading Cycle of the Experiment

4.0 EXPERIMENTAL RESULTS AND DISCUSSIONS

4.1 Force Deformation Behavior of Beams

Few small flexural cracks were marked at the end of Cycle-3 on the right end of the beam of Model 1 as shown in Fig.14. However, the cracks in beams were severe in Model 2 and flexural and flexural shear cracks were marked at the end of Cycle-4 as shown in Fig.16.Beam deflections are measured at the tip and beam slab joint of both the models. The deflection at the tip are shown here.

Fig 14. Model 1 Beam before Loading

Fig 15. Model 1 Beam Cracks after Loading

Beam secant stiffness are calculated from P-Δ hysteresis plots as shown in Fig.17 and 18. Secant stiffness is defined as the ratio of the strength to the maximum displacement. Secant stiffness of the beams for each load-deflection cycle is measured by considering the maximum load and deflection of forward and reverse loading of each cycle and it is found that beam stiffness decreases in each subsequent cycles.

Fig 15. Model 2 before Loading

Fig 16. Model 2 Beam Cracks

Model 1 lost stiffness showing an abrupt drop whereas Model 2 lost stiffness gradually in subsequent cycles as shown in Fig. 19. Theoretical plastic moment capacities of the beams are calculated and plotted with their P-Δ curve obtained from the experiment as shown in Fig.20.

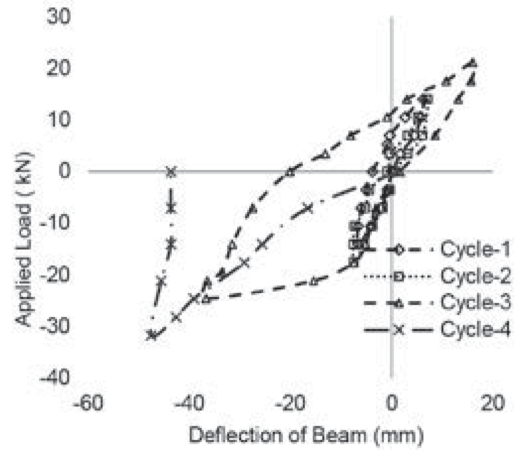

Fig 17. P-Δ Hysteresis Plot Beams Model 1

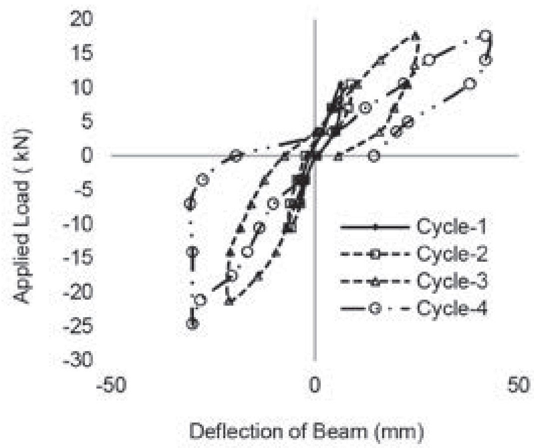

Fig 18. P-Δ Hysteresis Plot Beams Model 2

Performances of the beams in the present experiment are summarized in Table 3. It is found that beam of Model 2 exhibits better ductility than that of Model 1. The ductility of beam of Model 2 increased 46 %.

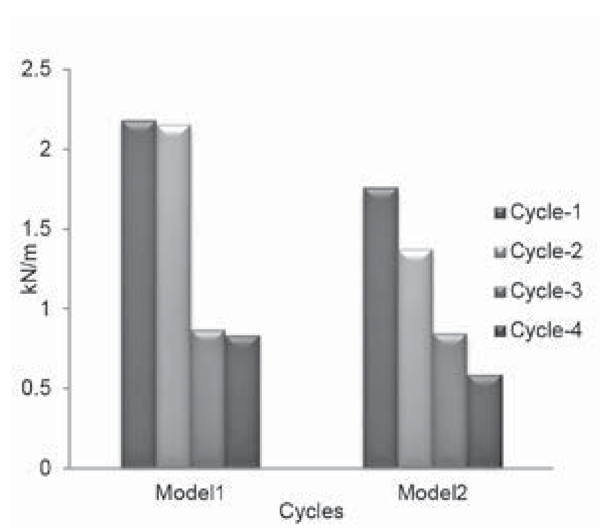

Fig 19. Stiffness of Beams

4.2 Force Deformation Behavior of Columns

Flexural and flexural-shear cracks developed in both upper and lower columns for both types of models under cyclic loading as shown in Fig.21 and Fig.23.

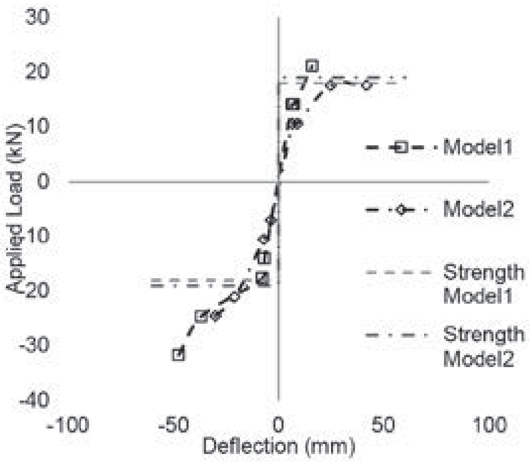

Fig 20. P-Δ behavior of Beams

Table 3. Ductility of Beams

Model No	First Crack		Condition of Failure		Ductility
	P (kN)	Δ (mm)	P (kN)	Δ (mm)	
Model 1	16	10.8	18.9	47.6	4.4
Model 2	10.5	6.5	17.6	42	6.46

Fig 21. Upper Column Failure, Model 1

Fig 22. Column of Model 2 before Loading

Fig 23. Column Failure, Model 2

From the load deflection hysteresis behavior of the columns, as shown in Fig.24 & 25, it is found that the column of Model 2 exhibited better ductile behavior as it deflected 30% higher than the column of Model 1 in forward loading and 26 % higher in reverse loading. Column deflection near the joint and at the tip were measured. Column secant stiffness were measured by considering maximum column shear and deflection for each cycle. Column shear is calculated from applied moment at the location of the dial gauge to measure the corresponding deflection. The computed stiffness is illustrated in Fig.26. It is found that, column of Model 2 lost stiffness gradually which indicates more ductile behavior. Plastic moment strengths of the columns are calculated and plotted with their P-Δ curve.

P-Δ curve of columns of Model 1 and Model 2 are shown in Fig.27. In forward cycle, both the samples experienced same column shear force but the column of Model 2 deflected 23% higher than column of Model 1. In reverse loading, column of Model 2, sustained 20% excess shear force while deflecting 22% higher than the column of Model 1. Column shear is calculated from the applied moment and corresponding deflection is measured. Performances of the columns are analyzed by the load-deflection hysteresis plots as shown in Fig.24 and 25.

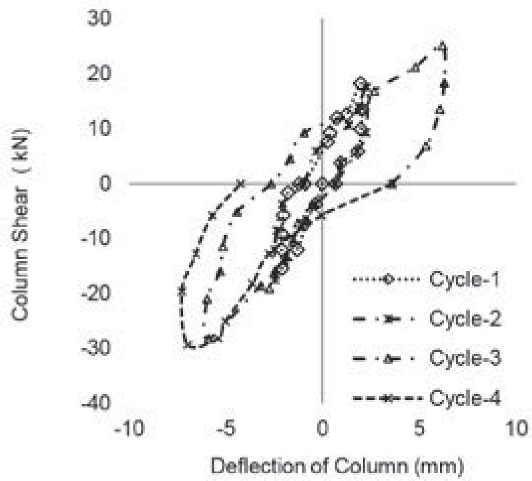

Fig 24. P-Δ Hysteresis Plot, Column (a) Model 1

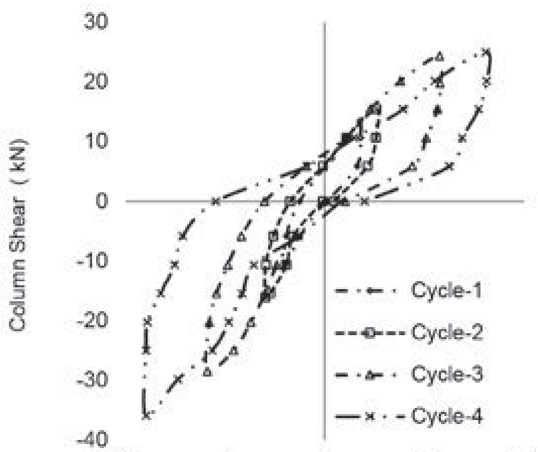

Fig 25. P-Δ Hysteresis Plot, Column Model 2

Column ductility is calculated from deflections measured at the appearance of the first crack and the deflection at failure. Performances of the columns in this experiment are shown in Table 4.

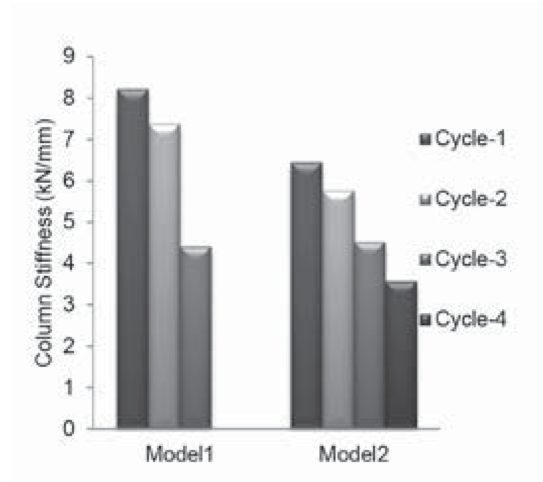

Fig 26. Column Stiffness

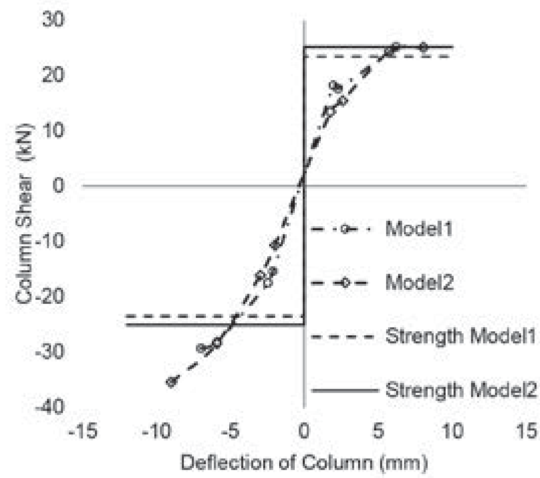

Fig 27. Load – Deflection Behavior of Column

It is found that Model 2 exhibits better ductility than that of Model 1. Column ductility was increased by 25% by increasing the concrete strength.

For both Model 1 and Model 2, ultimate failure occurred due to column failure while the beams were yet to reach their ultimate capacities. The column failed due the failure of the concrete by flexure-shear crack. It is observed from the experiment that in case of weaker column, the plastic hinge form in the column region. The beams were unable to transfer loads to the adjacent columns and the entire structure may collapse.

4.3 Moment-Rotation (M-Φ) Behavior of Joints

Rotation (Φ) experienced by the joints in each cycle depends on the magnitude of the applied moment, M. Rotations of the beams and columns at the joints against corresponding loading (applied moment) were measured by Video Extensometer.

Table 4. Ductility of Columns

Model No	First Crack		Condition of Failure		Ductility
	P (kN)	Δ (mm)	P (kN)	Δ (mm)	
Model 1	17.5	3.30	28	5.4	1.63
Model 2	15.44	5.6	36	11.4	2.03

Fig 28. Joint Failure of Model 1

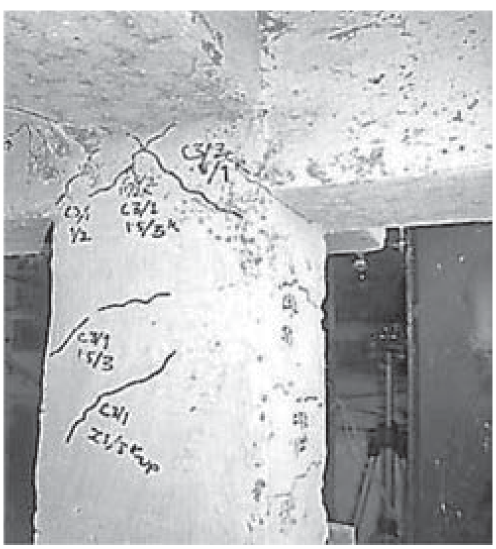

Fig 29. Joint Failure of Model 2

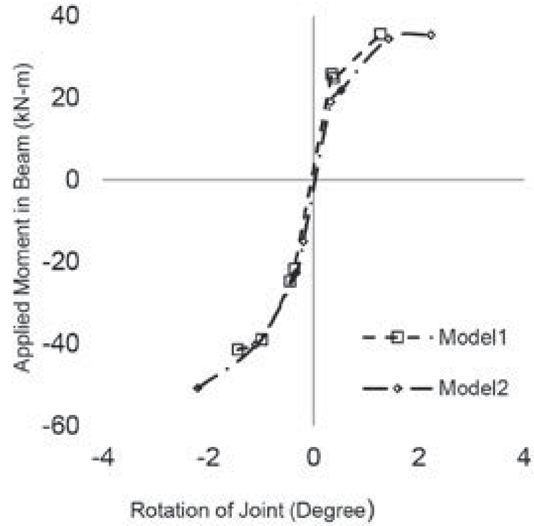

Fig 30. M-Φ behavior of Column Joint

Initially absolute rotation of the beam column joint was measured against time by video extensometer and relative rotations against the applied load and moment were calculated later. Both the joints exhibited diagonal shear cracks due to cyclic loading. Diagonal shear crack appeared in the first cycle in case of Model 1 whereas it appeared in the third cycle in case of Model 2. The cracks widened and propagated up to the transverse beams. Joint cracks approaching failure are shown in Fig. 23 and Fig.24. The difference in beam and column joints rotation is comparatively less within the elastic limit while the difference is greater in subsequent cycles. It is seen from the M-Φ curve that, beam and column joints of Model 2 rotates less against the same applied moment within the elastic limit whereas it rotates more than beam and column joint of Model 1 while approaching failure. It is found that, beam and column joint of Model 2 exhibit better ductility than the same of Model 1. Beam and column joint ductility increased by 68% and 136% respectively.

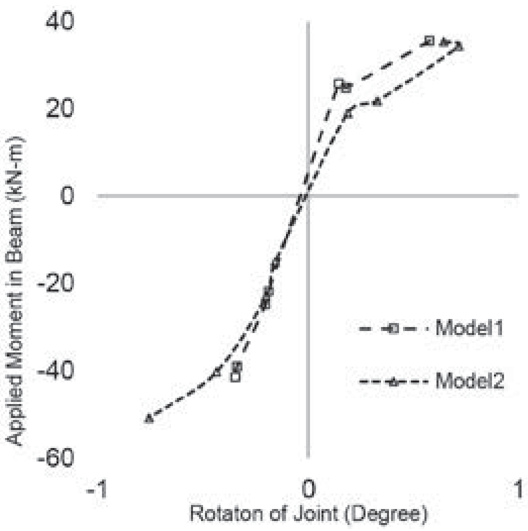

Fig 31. M-Φ behavior of Column Joint

5.0 CONCLUSIONS

It was observed that the beam, column and joint ductility increased due to the increased concrete strength. The joint exhibited better performance as the bond strength between the reinforcement and the concrete increased with increasing concrete strength. This experiment has shown ductility behavior of the structural member (beam, column and Joint) in case of varied concrete strength. In case of high strength concrete, the failure may be governed by reinforcement. The yield strength and elongation behavior of the steel reinforcement will govern the collapse behavior of the structure. A further study can be done by reinforcement failure. Following conclusions are drawn based on the experiment and analysis of the results:

a. Displacement ductility of the beam and column is increased by 46% and 25% respectively and rotational ductility of the beam and column joint is increased by 68% and 136% respectively by increasing the concrete strength from 18.31 MPa to 28.31 MPa i.e. 54% of the concrete strength.

b. Beam, column and joint stiffness of Model 2 decreased gradually under cyclic loading than Model 1. Therefore, concrete with high strength loses stiffness gradually under cyclic loading exhibiting better collapse behavior.

c. The experiments were carried out under some constrains. Only two models were prepared due to budget and labor constrain but it is found from the experiment that, ductility of the structural members i.e. beam, column and their joints increased with the higher concrete strength.A detail further study can be undertaken by preparing more number of models with low and high strength concrete and observing both concrete and reinforcement failure.

References:

[1] American Concrete Institute (ACI)-ASCE Committee 352. (2002). “Recommendations for Design of Beam-Column Connections in Monolithic Reinforced Concrete Structures.” ACI 352R-02, Farmington Hills, MI.

[2] American Concrete Institute (ACI) Committee 318. (2002). “Building code requirements for structural concrete and commentary.” ACI 318-02 and ACI 318R-02, Farmington Hills, MI.

[3] Akguzel,U., and Pampanin, S. (2007). “Seismic Response of RC Beam-Column Joints Upgraded with FRP Sheets. II: Analysis and Parametric Study.” ASCE, Journal of Composites for Construction, Vol. 11, No 6, pp. 590-600.

[4] Akguzel, U., and Pampanin, S. (2012). “Assessment and Design Procedure for the Seismic Retrofit of Reinforced Concrete Beam-Column Joints using FRP Composite materials.” ASCE, Journal of Composites for Construction, Vol. 16, No 1, pp. 21-34.

[5] Cosgun, Cumhur.,Comert, Mustafa., Demeir, Cem., and Ilki, Alper. (2012). “ FRP Retrofit of a Full Scale 3D RC Frame,” Istanbul Technical University.

[6] Eligehausen, R., Popov, E.P., and Bertero, V.V. (1983) “Local Bond Stress-slip Relationships of Deformed Bars under Generalised Excitations.”Report UCB/EERC-83/19, Earthquake Engineering Research Center, University of California, Berkeley, 178p.

[7] Federal Emergency Management Agency (FEMA). (1997). “NEHRP Guidelines for Seismic Rehabilitation of Buildings October.” FEMA 273.

[8] Hakuto, S., Park, R., and Tanaka, H. (2000). “Seismic Load Tests on Interior and Exterior Beam-Column Joints with Substandard Reinforcing Details.” Structural journal, ACI, 97(1), pp11-25.

[9] Ichinose, T. (1991). “Interaction between Bond at Beam Bars and Shear Reinforcement in RC Interior Joints, Design of Beam-Column Joints for Seismic Resistance.” SP-123, American Concrete Institute, Farmington Hills, Mich., pp. 379-400.

[10] Leon, R.T. (1990). “Shear Strength and Hysteretic Behavior of Beam-Column Joints,” ACI Structural Journal, Jan-Feb, vol.87, No.1, pp. 3-11.

[11] .Nilson., H Arthur. (1997). “Design of Concrete Structures.” 12 Edition, chap 10, pp 332-358, The McGraw-Hill Companies, Inc, New York.

[12] Neville, A.M. (1995). “Properties of Concrete,” chap 3, pp 108-120, 4th Edition, Pearson Education, Inc, Nodia, India.

[13] Prota, Andreas.,Nanni , Anotnia., Gaetano, Manfredi., and

Cosenza, Edoward. (2004). “Selective upgrade of under Designed Reinforced Concrete Beam-Column Joints Using Carbon Fiber Reinforced Polymers.” ACI Structural Journal, Sep-Oct vol 101, No 5, pp 699-707.

[14] Paulay, T., and Priestley, M.J.N. (1992).“Seismic Design of Reinforced Concrete and Masonry Buildings,” John Wiley publications New York.

[15] Uma, S.R., and Prasad, A.Meher., (2005). “Seismic Behavior of Beam Column Joints in Reinforced Concrete Moment Resisting Frames.” document no IITK-GSDMA-EQ-31-V1-0, IITK-GSDMA Project on Building Code.